THE JOURNAL OF PHYSICAL CHEMISTRY B

Article

pubs.acs.org/JPCB

# Speciation of Copper–Peptide Complexes in Water Solution Using DFTB and DFT Approaches: Case of the [Cu(HGGG)(Py)] Complex

Maurizio Bruschi,*[,§] Luca Bertini,[†] Vlasta Bonačić-Koutecký,[‡] Luca De Gioia,[†] Roland Mitrić,[¶] Giuseppe Zampella,[†] and Piercarlo Fantucci*[,†]

[†]Department of Biotechnologies and Biosciences, University of Milano-Bicocca, Piazza della Scienza 2, I-20126 Milano, Italy

[‡]Institut für Chemie, Humboldt-Universität zu Berlin, Brook-Taylor-Strasse 2, D-12489 Berlin, Germany

[§]Department of Environmental Science, University of Milano-Bicocca, Piazza della Scienza 1, I-20126 Milano, Italy

[¶]Fachbereich Physik, Freie Universität zu Berlin, Arnimallee 14, D-14195 Berlin, Germany

**ABSTRACT:** The DFTB and DFT methods are applied to the study of different forms of the [Cu(HGGG)(Py)] complex in water, with the aim of identifying the most stable isomer. The DFTB calculations were possible thanks to a careful parametrization of the atom–atom repulsive energy terms for Cu–H, Cu–C, Cu–N, and Cu–O. The speciation process is carried out by computing different DFTB-steered molecular dynamics (SMD) trajectories, each of which ends in a well-defined different form. The last frame of each trajectory is subjected to geometry optimization at both DFTB and DFT levels, leading to a different isomer. From the corresponding energy values, a rank of relative stability of the isomers can be established. The computational protocol developed here is of general applicability to other metal–peptide systems and represents a new powerful tool for the study of speciation of metal-containing systems in water solution, particularly useful when the full characterization of the compound cannot be carried out on the basis of experimental results only.

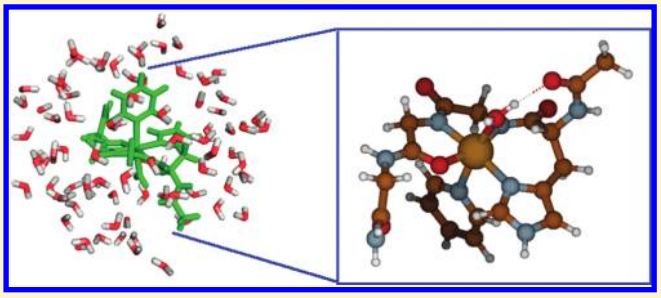

## 1. INTRODUCTION

The problem of speciation of metal–peptide complexes arises from two essential features of the peptide ligand: the high flexibility of the amino acid chain, particularly in the absence of relevant intramolecular H-bonds, and the occurrence along the amino acid chain of multiple chemical groups able to act as ligands.[1−3] We mention the anionic sites such as the deprotonated –NH amidic groups, the carboxylate group of Glu and Asp, and the neutral ligand sites (N donor) in His, Arg, and Lys. In addition, it is proved from X-ray diffraction studies[4] that also the oxygen atom of the carbonyl group can act as a ligand. To the high number of possible ligand sites in the peptide corresponds a relatively low coordination number that the metal ion, in particular Cu(II), can assume. It is indeed frequent to have coordination numbers equal to 4 or 5 with one of the coordination sites potentially occupied by one water molecule of the solvent. It is easy to figure out that for peptides with 5 or 6 residues of the type described above, few tenths of possible isomers are possible. Fortunately, some specific coordination modes do produce steric hindrances in the chain and consequently help in reducing the manifold of possible isomers. A further constraint can result from the fact that coordination of ligand sites in contiguous amino acids can lead to the formation of stabilizing 5- or 6-membered rings. Coordination of ligand sites distant in the chain is less probable when it induces strain in the peptide, but, in particular instances, can allow a specific ligand to switch from axial to equatorial position, thus further incrementing the number of possible forms. Even considering constraints and general rules for preferred coordination modes, and even taking into account the indications given by X-ray diffraction studies, the number of possible stable forms accessible to a metal–peptide complex in water solution still remains very large. It is therefore difficult to predict in an unambiguous way the shape of a metal–peptide complex, and also the experimental measurements may be unable to solve completely the problem. Sources of experimental data, in water solution, related to the coordination mode of paramagnetic metal ions are actually limited to the EPR (hyperfine coupling constants and to a smaller extent g tensor values), or UV–vis spectroscopy, which is even less predictive than EPR.[5−10] In this context, it would be very valuable to have any help from theoretical methods to support hypothesis formulated on the basis of experimental data. However, one has to consider the fact that metal–peptide complexes in water solution are, by definition, large and complex systems, which evidently limit the accuracy of the computational methods to be employed. In this respect, the field of the classical mechanics force-field-based methods is

**Received:** October 29, 2011
**Revised:** April 25, 2012
**Published:** April 26, 2012

  

largely unexplored for metal complexes, and the semiempirical methods of the NDDO family seem to be characterized by a predictive capability satisfactory only at a qualitative level.[11] The most convenient quantum mechanical approach that could be employed in the field of speciation of complex metal systems seems to be the density function theory in the formulation of the tight-binding approximation (DFTB) which has been proposed in the recent years.[12−16] This method is characterized by a well-defined theoretical structure and by a clear connection with the ab initio method from which it is derived. The DFTB approach proved to be a reliable predictive tool for large chemical systems such as bulk or nanoparticle aggregates,[17−23] and biologically relevant molecules.[24−28] In the field of bioinorganic molecules, the number of DFTB studies so far reported is small.[26,29−37] When the necessary parametrization is available for specific atoms, the DFTB method shows a satisfactory accuracy, while requiring computational times at least 2 or 3 orders of magnitude shorter than the DFT methods. As a consequence, DFTB seems to be a very appealing procedure just for large systems.

In this paper, the DFTB method is employed as a part of a new computational protocol for the study of speciation of metal−peptide complexes in water solution. We considered, as an example, the Cu(II) complex [Cu(HG$_1$G$_2$G$_3$)(Py)(W)] (H = histidine, G = glycine, Py = pyridine and W = $H_2O$), which contains the species [Cu(HG$_1$G$_2$G$_3$)] related to compounds formed by the interaction of the $Cu^{2+}$ ion with the prion protein and its modification toward a pathological configuration. Such copper−peptide systems have been the subject of other theoretical[38−43] and experimental studies.[4,8−10,44−50] The complex we have chosen to study includes also two potential ligands (Py and W) external to the peptide. The possible influence of such additional ligands has been investigated experimentally by EPR and UV−vis spectroscopies.[10]

The core of our computational protocol is represented by the DFTB steered molecular dynamics (SMD) combined with standard DFT calculations. Each SMD trajectory ends in a particular form, usually very close to an isomer, and this allows a systematic and complete investigation of the manifold of isomers. All the SMD trajectories are initiated from a common precursor (a six-coordinated complex) in which one or two copper−ligand bonds are progressively dissociated. The last frame of each SMD trajectory can be subjected to DFTB geometry optimization, leading to the identification of real isomers and their relative stabilities. In order to improve the predictive capability of the procedure, the geometry optimization is carried out also at DFT level. The comparison between DFTB and DFT results for minimum-energy structures allows also a direct assessment of the reliability of the DFTB approach for this class of molecular systems.

The copper−peptide systems here considered, are composed of 60 atoms, and a minimal representation of the solvation sphere requires 84 water molecules. For such systems, a medium-quality basis set (for all-electron calculations) has dimension larger than 3000. The corresponding DFT calculations are very demanding, and the problem can be alleviated by just combining the rigorous DFT method with a simplified DFTB version.

It should be stressed again that the DFTB calculations are possible only if accurate parametric potentials for atom−atom interactions are available. The determination of such potentials, which has never been worked out before for copper−ligand pairs, is a qualifying point of the present study.

As is well-known, the DFTB Hamiltonian is based on two-center contributions of electronic and repulsive character, respectively (see next section). The first contribution can be easily computed once the basis set for valence electrons is chosen, while the second contribution is more complicated due to the following reasons. The atom−atom repulsive energy term, as it appears in the standard form of the DFTB Hamiltonian, is actually composed of different *effective* contributions which are not clearly defined, and which consequently cannot be computed theoretically. Therefore, the atom−atom repulsive terms must be considered as the *empirical* part of the method, and it is usually determined in such a way that DFTB results closely mimic the DFT (ab initio) results. In the present study, the standard DFTB atom−atom potentials[12,51] have been adopted for all nonmetal atoms, while a new determination of the atom−atom repulsive terms is carried out for the pairs Cu−H, Cu−C, Cu−N, and Cu−O, which cover all cases relevant for the copper−peptide complexes (with the exclusion of the sulfur-containing amino acids).

The paper is organized as follows. In the next section, the computational methods adopted are outlined. In particular, we will present the way used to optimize the atom−atom repulsive DFTB potentials and discuss their ability to reproduce the best geometries (obtained at DFT level) of a set of reference simple copper-containing molecules. The reliability of the DFTB atom−atom repulsive terms is further checked for a small set of copper containing complexes which have been computed also at DFT level. Then, the protocol used for DFTB-SMD simulations necessary for the speciation of a copper−peptide complex in water solution will be discussed. Section 3 reports the results obtained by applying the procedure outlined in section 2 on the copper−peptide complex [Cu(HGGG)(Py)-(W)], a six-coordinated species which is used in the present context only as the precursor of all possible five- and four-coordinated species, obtained by means of SMD simulations, along which one or two copper−ligand bonds are dissociated.

## 2. COMPUTATIONAL METHODS

**2.1. Optimization of the DFTB Repulsive Potentials.** Following the original formulation of the spin-polarized self-consistent-charge DFTB method,[12−16] as implemented in the DFTB+ code,[15] the energy expression for a molecule, (valence electrons only), can be written in the form:

$$E = \sum_{\alpha} f_{\alpha} \sum_{\lambda\mu} C_{\lambda\alpha} C_{\mu\alpha} H^{0}_{\mu\lambda} + \frac{1}{2} \sum_{IJ} \gamma_{IJ} \Delta q_I \Delta q_J + \frac{1}{2} \sum_{I} \sum_{\sigma\sigma'} p_{I\sigma} p_{I\sigma'} W_{I\sigma\sigma'} + \sum_{I<J} V^{\mathrm{rep}}_{IJ}(r_{IJ})$$

$$E = E_{\mathrm{el}} + E_{\mathrm{rep}} \qquad (1)$$

where $\hat{H}^{0}_{\mu\lambda}$ is the Kohn−Sham Hamiltonian which depends only on the reference electron densities on atoms, $C_{\lambda\alpha}$ are the (real) coefficients of the one electron functions in terms of the basis functions $\phi_\alpha = \sum_\lambda C_{\lambda\alpha}\chi_\lambda$, and $\gamma_{IJ}$ is the two-center interaction parameter which multiplies the distortion of the electron densities $\Delta q_I$, $\Delta q_J$ on the atoms $I$ and $J$, respectively. The spin densities associated with the valence shells $\sigma$ and $\sigma'$ on the atom $I$ ($p_{I\sigma}$ and $p_{I\sigma'}$, respectively) interact via the one-center parameter $W_{I\sigma\sigma'}$. Finally, the last term of eq 1 is the two-center repulsion term. In principle, such a contribution could be derived considering reference energy data computed at DFT


dx.doi.org/10.1021/jp210409c | J. Phys. Chem. B 2012, 116, 6250−6260

(ab initio) level. For instance, for a simple diatomic XY, the repulsive term $V_{XY}^{rep}(R_{XY})$ could be derived from the following relation:

$$V_{XY}^{rep}(R_{XY}) = E^{DFT}(R_{XY}) - E_X^{DFT} - E_Y^{DFT} - (E^{DFTB}(R_{XY}) - E_X^{DFTB} - E_Y^{DFTB})$$

where DFT and DFTB label the reference ab initio and the approximate values, respectively. However, according to our experience, such a procedure gives unsatisfactory results when applied to simple Cu−Y (Y = H, C, N, O) diatomics because the corresponding DFTB results for best molecular geometries are significantly different from the DFT reference ones. Therefore, we have chosen to proceed according to the following protocol:

(i) The best molecular geometries for a series of simple copper-containing systems are determined at the DFT level using the BP86 exchange-correlation functional[52,53] and the triple $\zeta$ plus polarization basis set TZVP[54] implemented in the Turbomole 5.9 suite of programs.[55] The reference set of (closed shell) molecules is composed of the following 13 species: $[CuCO]^+$, CuCN, $[Cu(CN)_2]^+$, $CuCH_3$, $CuNH_2$, $[CuNH_3]^+$, $[Cu(NH_3)_2]^+$, $CuNO_3$, CuOH, $[CuOH_2]^+$, $[Cu(OH_2)_2]^+$, $CuOCH_3$, and $[CuOCH_2]^+$. The corresponding best atomic coordinates for each species M are collected into the vector $\mathbf{r}_M^{DFT}$.

(ii) The repulsive potentials to be optimized are the following: $V_{CuY}^{rep}$ (Y = H, C, N, O). As done in the standard Slater−Koster files,[12,51,56,57] each potential $V_{CuY}^{rep}(R_{CuY})$ is represented by piecewise cubic splines in the range $[r_{CuY}^0, (r_{CuY}^{cutoff} - \delta r)]$ with a step $\delta r$. For $R_{CuY} < r_{CuY}^0$ the potential is represented by an exponential function, in the interval $[(r_{CuY}^{cutoff} - \delta r), r_{CuY}^{cutoff}]$ the potential is expressed as a fifth-order polynomial, with the condition $V_{CuY}^{rep}(r_{CuY}^{cutoff}) = 0$, together with the associated null first and second derivatives.

(iii) For a given form of each $V_{CuY}^{rep}$ (Y = H, C, N, O) potential, the geometries of the 13 reference molecules are optimized at DFTB level and the corresponding best coordinates are collected into $\mathbf{r}_M^{DFTB}$ ($M$ = 1,2,...,13). The optimum definition of the repulsive potentials comes from the minimization of the fitting error

$$Z = \sum_M |\mathbf{r}_M^{DFT} - \mathbf{r}_M^{DFTB}| \quad (2)$$

Let $[V_{CuY}^{rep}(R_{CuY})]_0$ be the initial (guess) form and $V_{CuY}^{rep}(R_{CuY})$ the current form of the potential to be optimized. $V_{CuY}^{rep}$ is iteratively modified according to $V_{CuY}^{rep}(R_{CuY}) = [V_{CuY}^{rep}(R_{CuY})]_0 + V_{CuY}^{LJ}(R_{CuY})$, where $V_{CuY}^{LJ}(R_{CuY}) = -A_{CuY}/R_{CuY}^6 + B_{CuY}/R_{CuY}^{12}$, using the Lennard-Jones $A_{CuY}$ and $B_{CuY}$ parameters as well as the cutoff distances $r_{CuY}^{cutoff}$ as free variables. Therefore, for the set of Cu−H, Cu−C, Cu−N, and Cu−O potentials we have a total of 12 variables on which the DFTB energies and best geometries depend. The minimization of $Z$ (eq 2) $Z = f(\{A_{CuY}, B_{CuY}, r_{CuY}^{cutoff}$, Y = H, C, N, O$\})$ is achieved by means of several heating−cooling cycles of fast simulated annealing.[58] This gives us confidence that the determined potentials have a form close to the global optimum. The best DFTB molecular geometries corresponding to the best repulsive potentials compare with the DFT ones in a very satisfactory manner, as it will be shown in the next section.

In all of the present calculations the DFTB parameters for the pairs of atoms formed by H, C, N, and O are those of the mio-0-1 set available at www.dftb.org.[12,51] For the case of Cu−X (X = Cu, H, C, N, O) the electronic part has been computed for each diatomic on a suitable grid of points. The atomic calculations have been carried out using ad hoc developed atomic program derived from the original Clementi's code.[59] Calculations were performed on extended basis sets of Slater orbitals, using the PBE exchange-correlation functional,[60,61] and values for $r_0$ parameter defining the confining potential equal to 4.2, 3.0, 2.7, 2.2, and 2.3 Bohr for Cu, H, C, N, and O, respectively.

**2.2. DFTB-Steered Molecular Dynamics and the Generation of the Low-Energy Configurations of a Copper−Peptide Complex in Water Solution.** The description of the methodology we will present here refers to the specific case of the $[Cu(HG_1G_2G_3)(Py)(W)]$ complex (see also next sections) which has been used as a test case. However, our protocol is of general applicability to other metal complexes, for which the explicit treatment of the water solvent is required.

The identification of the best isomer for a copper−peptide complex may be considered as an interesting example of the general problem of speciation of complexes in water solution. In our case, such a problem can be formulated as follows. The $Cu^{2+}$ ion interacting with the peptide $HG_1G_2G_3$ is coordinated by two deprotonated amidic −NH groups of glycine residues $G_1$ and $G_2$, by the nitrogen atom of the histidine residue (H), and by the carbonyl oxygen atom of the glycine $G_2$. In water solution and in the presence of a pyridine ligand, the coordination sphere can be expanded including the nitrogen atom of pyridine $N_{Py}$ and the oxygen atom of a water molecule acting as coordinating solvent $O_W$. The six-coordinated complex $[Cu(HGGG)(Py)(W)]$ (hereafter referred as **0**) plays the role of a precursor of all other possible forms (see section 3) the formation of which is simulated by means of steered molecular dynamics (SMD) calculations. Along a particular SMD trajectory, starting from **0**, the Cu−Y bond (or the bonds Cu−Y and Cu−Y′) is progressively elongated by applying a force along the line Cu−Y and acting in opposite directions on Y and Cu, respectively. In particular, if at time $t$ $\mathbf{n}$ is the unit vector $\mathbf{n}(t) = [\mathbf{r}_Y(t) - \mathbf{r}_{Cu}(t)]/R_{CuY}(t)$, the force acting on Y and Cu, respectively, may be defined as

$$\mathbf{f}_Y(t) = \mathbf{n}(t)F(\bar{R}_{CuY} - R_{CuY})$$

$$\mathbf{f}_{Cu}(t) = -\mathbf{f}_Y(t) \quad (3)$$

where $\bar{R}_{CuY}$ is an upper or lower limit for the Cu−Y distance at which the bond is considered as completely dissociated or formed. The scalar $F$ is set equal to a value large enough to promote the dissociation or formation of the bond (e.g., 0.005 hartree/bohr) within the time scale used for our simulations (15 ps). Equation 3 is valid for both bond dissociation ($\bar{R}_{CuY}$ set equal to 5 Å) and bond formation ($\bar{R}_{CuY}$ set equal to 2.5 Å). During the simulations, the additional forces can be switched on and off depending on the actual behavior of the considered copper−ligand bond. $F$ is set equal to zero when $R_{CuY} \geq \bar{R}_{CuY}$ for bond dissociation or when $R_{CuY} \leq \bar{R}_{CuY}$ for bond formation. The SMD simulations are carried out considering all water molecules as free with the exception of the few ones within 1 Å from the surface of the hydration sphere, which are constrained to their original position (see below).

In order to avoid that during the SMD simulation the system could overcome an energy barrier leading to the dissociation of a bond different from that considered, the SMD trajectory is computed at low temperature. This corresponds, in practice, to a geometry minimization carried out in the presence of additional forces. The end point of the SMD (low temperature) trajectory is in general very close to a specific isomer and it can be used for a further refinement, using DFTB or DFT optimizations. As an alternative, one could run higher temperature SMD by imposing that one or two Cu−Y bonds are dissociated while other four coordination bonds are forced to be formed.

**2.3. Optimization of the Structures of the Isomers Starting from the Final Configurations of the SMD Simulations.** The last frame of the SMD trajectory for each different form of the copper−peptide complex is used as the starting point for geometry optimizations carried out at DFTB and DFT levels. The best DFTB geometries are obtained as the lowest energy frame of an additional 10 ps MD simulation at $T$ = 1 K, followed by a gradient based optimization. The DFT geometry optimizations are carried out using the PB86 functional[52,53] and the TZVP basis set[54] for all atoms. The considered copper−peptide complexes (see below) are composed by 60 atoms and surrounded by 84 water molecules. The size of the TZVP basis set for such a system is larger than 3300, a number which makes the DFT geometry optimizations very time consuming. In particular, when all Cartesian coordinates are optimized, in the presence of an extended network of fluxional H-bonds, the convergence is very slow, with an oscillating behavior of gradients. This aspect needs to be carefully investigated in the future to make the protocol here designed applicable to other systems in a very effective way.

The DFTB or DFT total energy ($E_T$) of the investigated systems composed by the copper complex [Cu(HGGG)(Py)(W)] and by the water molecules can be partitioned in the sum of the three energy terms

$$E_T = E_C + E_{C-W} + E_{W-W}$$

where $E_C$, $E_{C-W}$, and $E_{W-W}$ are the energies of the complex, its hydration energy, and the energy of the solvent sphere. In order to indentify the most stable isomer we need to obtain the $E_C + E_{C-W}$ sum of energies, which is equal to $E_T - E_{W-W}$. Clearly, it is impossible to separate the three contributions from a single DFT energy value because the density of each subsystem depends on the densities of all other subsystems. However, it is possible to estimate the $E_{W-W}$ by repeating a single SCF calculation on the water sphere in which the atoms are frozen in the best complex−water geometry.

## 3. RESULTS

**3.1. Optimization of the Cu−Y Pair Repulsive Potentials.** As mentioned above, the set of reference molecules used to optimize the pair repulsive potentials is composed of the 13 closed-shell species, reported in Table 1, which are representative of all the features of copper−ligand bonds occurring in copper−peptide complexes. The species $[CuOCH_2]^+$ is representative of the bond between copper and an oxygen carbonyl atom of a formaldehyde, a situation occurring in our complex [Cu(HG$_1$G$_2$G$_3$)(Py)(W)] for the second glycine residue.

The data of Table 1 concerning the best Cu−Y DFTB distances compare well with those of the corresponding DFT (TZVP/BP86) calculations. The agreement is equivalent to or better than that reported for other transition metal compounds.[56] The numerical data defining the pair repulsive potential in the format of standard Slater−Koster files are available on request.

**Table 1. Cu−Y Distances for Molecules of the Reference Set, Obtained with Optimized DFTB Pair Repulsion Potentials of Cu−H, Cu−C, Cu−N, and Cu−O, Compared with the Corresponding DFT (TZVP/BP86) Results[a]**

| molecule | Cu−Y | Cu−Y distances |
|---|---|---|
| $[CuCO]^+$ | Cu−C | 1.867 (1.840) |
| | Cu−O | 2.979 (2.972) |
| CuCN | Cu−C | 1.867 (1.817) |
| | Cu−N | 3.021 (2.991) |
| $[Cu(CN)_2]^-$ | Cu−C | 1.867 (1.895) |
| | Cu−N | 3.019 (3.067) |
| $CuCH_3$ | Cu−C | 1.867 (1.894) |
| | Cu−H | 2.505 (2.468) |
| $CuNH_2$ | Cu−N | 1.909 (1.830) |
| | Cu−H | 2.552 (2.328) |
| $[CuNH_3]^+$ | Cu−N | 1.909 (1.918) |
| | Cu−H | 2.497 (2.494) |
| $[Cu(NH_3)_2]^+$ | Cu−N | 1.909 (1.921) |
| | Cu−H | 2.498 (2.501) |
| $CuNO_3$ | Cu−N | 2.394 (2.465) |
| | Cu−O$_1$, Cu−O$_2$ | 2.011 (2.074) |
| | Cu−O$_3$ | 3.595 (3.682) |
| CuOH | Cu−O | 1.787 (1.806) |
| | Cu−H | 2.383 (2.291) |
| $[CuOH_2]^+$ | Cu−O | 1.908 (1.922) |
| | Cu−H | 2.588 (2.615) |
| $[Cu(OH_2)_2]^+$ | Cu−O | 1.910 (1.902) |
| | Cu−H | 2.586 (2.590) |
| $CuOCH_3$ | Cu−O | 2.010 (2.008) |
| | Cu−C | 2.980 (2.971) |
| | Cu−H$_1$ | 2.951 (2.966) |
| | Cu−H$_2$, Cu−H$_3$ | 3.717 (3.707) |
| $[CuOCH_2]^+$ | Cu−O | 1.848 (1.889) |
| | Cu−C | 2.891 (2.932) |
| | Cu−H$_1$ | 3.235 (3.264) |
| | Cu−H$_2$ | 3.848 (3.874) |

[a]Distances in Å; DFT distances are reported in parentheses.

When compared with the ab initio results, the errors affecting the DFTB values for Cu−Y distances are acceptably small. The distances representing direct coordination bonds are in error by (1−3) × $10^{-2}$ Å, while a little larger discrepancy occurs for nonbonded Cu−Y distances, due to errors affecting the Cu−X−Y angles.

The accuracy with which our DFTB Cu−Y repulsive potentials reproduce DFT best geometries (as well as experimental geometries) has been further checked in the case of three copper complexes, namely copper−bis(ethylendiamine) $[Cu(en)_2]^{2+}$, copper−bis(acetylacetonate) $[Cu(acac)_2]$, and copper−bis(glycinate) $[Cu(gly)_2]$. The DFT results are obtained using both BP86[52,53] and B3LYP[62] functionals with the TZVP basis set. The results of such a comparison are reported in Table 2. The disagreement between the DFTB and the DFT results is slightly larger than that computed for the compounds of Table 1, but still very acceptable. Also the valence angles involving the copper atoms are predicted from the DFTB approach in a very satisfactory manner. These results obtained for open-shell systems (which


dx.doi.org/10.1021/jp210409c | J. Phys. Chem. B 2012, 116, 6250−6260

**Table 2. Selected Geometrical Parameters (Distances in Å, and Angles in deg) of Model Cu Complexes Calculated at Different Levels of Theory**

| | $[Cu(en)_2]^{2+}$ | | |
|---|---|---|---|
| | Cu−N | N−Cu−N | Cu−N−C |
| TZVP/BP86 | 2.069 | 83.6 | 108.8 |
| TZVP/B3LYP | 2.071 | 83.5 | 108.8 |
| DFTB | 1.995 | 83.8 | 110.5 |
| expt[a] | 2.012, 2.019 | 84.7 | 108.3, 108.6 |
| | $[Cu(acac)_2]$ | | |
| | Cu−O | O−Cu−O | Cu−O−C |
| TZVP/BP86 | 1.954 | 92.9 | 125.9 |
| TZVP/B3LYP | 1.955 | 88.9 | 129.1 |
| DFTB | 2.010 | 91.7 | 125.8 |
| expt[b] | 1.912, 1.914 | 93.2 | 125.9, 126.0 |

| | $[Cu(gly)_2]$ | | | | |
|---|---|---|---|---|---|
| | Cu−N | Cu−O | O−Cu−N | Cu−N−C | Cu−O−C |
| TZVP/BP86 | 2.040 | 1.929 | 85.8 | 108.9 | 117.0 |
| TZVP/B3LYP | 2.048 | 1.909 | 85.6 | 108.4 | 118.0 |
| DFTB | 1.906 | 2.010 | 85.5 | 114.2 | 114.2 |
| expt[c] | 1.984 | 1.957 | 85.4 | 109.5 | 115.9 |

[a]Taken from ref 67. [b]Taken from ref 68. [c]Taken from ref 69.

are absent in the reference set of Table 1) suggest that the pair repulsive potentials we worked out can be effectively used in simulations of copper−peptide complexes.

**3.2. Speciation of Copper−Peptide Complexes in Water Solution.** The computational procedure outlined in section 2, together with the optimized $V_{CuY}(R_{CuY})$ potentials, has been applied to the speciation of the $[Cu(HG_1G_2G_3)(Py)(W)]$ complex in water solution. The need for theoretical investigation of the speciation of such a system is connected with the fact that an unambiguous definition of the formulation of copper−peptide complex in water is a difficult task also from an experimental point of view. The experimental determination of the coordination form of the complex is commonly based on its EPR data (especially hyperfine constants with $^{53}Cu$ and $^{14}N$, and $g$ values). However, due to the presence of water which can act as coordinating solvent, the experimental data cannot rule out the hypothesis that a water molecule is coordinated (in an axial or equatorial position). In addition, the water molecule can interact with the copper atom in a quite weak manner, being held in the right position because of a network of H-bonds in which it is involved. The presence of a *semi-coordination* of a water molecule in copper−peptide complexes caused by H-bonds has been shown also by X-ray diffraction experiments.[4,63]

The possible formation of an extended network of H-bonds among the complex and the water molecules has a severe impact on the theoretical model needed for studying such systems. In particular, the following points must be taken into account: (i) the solvent must be treated in an explicit manner, due to the possible dual role of solvent and ligand played by water molecules; (ii) the H-bond network has an intrinsic fluxional behavior, which cannot be described in terms of a single structure, a fact requiring the use of a MD approach; and (iii) the number of water molecules explicitly considered must be sufficiently high to ensure that all the polar sites of the peptide are properly hydrated.

All these aspects have never been considered in previous theoretical studies on copper−peptide complexes. In this sense, our approach, a combination of DFTB-SMD and DFT calculations, seems to be a substantial step forward in the speciation of copper species in solution.

As mentioned above, the main aim of our study is to show how the process of speciation can be carried out. To this end, we have chosen as a reference a six-coordinated complex in which Cu(II) interact with the peptide $AcHG_1G_2G_3NH_2$, which is acetylated in the first histidine residue and amidated at the last glycine residue, and which provides four coordination points: the nitrogen of histidine ($N_H$), the deprotonated H−N amidic groups of $G_1$ and $G_2$ ($N_{G1}$, $N_{G2}$), and the carbonyl oxygen of $G_2$ ($O_{G2}$). A pyridine ligand Py ($N_{Py}$) and a water molecule ($O_W$) may complete the coordination sphere. The searching for the best isomer has been subjected to the following constraints: (i) in all forms the two deprotonated H−N groups are present (thus providing the charge neutrality of the system); and (ii) when coordinated, the pyridine and water ligands always occupy axial positions, and therefore, $N_H$, $N_{G1}$, $N_{G2}$, and $O_{G2}$ occupy equatorial positions.

These constraints can be removed to make the speciation procedure completely general, that is based on all the six-coordinated species (see Table 3), which obey, however, to the rule that only the first residue H can be displaced from equatorial to axial position, in order to avoid internal distortion into the rest of the peptide. Correspondingly, either the W or the Py ligand (but not both) can occupy equatorial positions. In the present study, only the first six-coordinated form of Table 3 (labeled as **0**) has been used to generate all the isomers (labeled **1**, **2**, ..., **10**). The global speciation based on all the precursors of Table 3 will be the subject of a forthcoming paper.

*Six-Coordinated Form.* The structure of the six-coordinated form **0** used as the precursor is reported in Figure 1. In order to simulate the hydration process, the species **0** has been located at the center of a sphere of 84 water molecules: the whole system is therefore composed of 312 atoms, 252 belonging to the hydration sphere and 60 to the complex (including the pyridine ligand and a coordinating water molecule).

The species **0** has been proved not to be a real isomer, both at DFTB and DFT level. In the presence of an axially coordinated pyridine ligand, the water molecule tends to dissociate when the structure of **0** is optimized in vacuo or to be located at large distance from copper atom (>3.5 Å), when optimized within the water sphere. The agreement, at least at qualitative level, between DFTB and DFT methods concerning the nonexistence of a six-coordinated form is encouraging. In this respect, we would like to mention that the semiempirical SAM1D Hamiltonian[64,65] implemented in the AMPAC package[66] reaches a stationary point for **0**, confirming the observation we made for several other copper−peptide complexes that such a procedure favors coordination numbers higher than those given by more rigorous methods. Due to its intrinsic instability, the six-coordinated species **0** used in our simulations has been actually obtained as a constrained form, by means of a 15 ps DFTB SMD simulation in which all the six copper−ligand bonds are forced not to be larger than 2.5 Å.

*Five-Coordinated Forms.* Under the assumption that $N_{G1}$ and $N_{G2}$ are always coordinated (see above), the precursor **0** can generate four different five-coordinated forms, which are reported in Table 3, corresponding to the dissociation of Cu−$N_H$ (**1**), Cu−$O_{G2}$ (**2**), Cu−$N_{Py}$ (**3**), and Cu−$O_W$ (**4**), respectively. All the four species **1**−**4** are the end points of low-temperature DFTB SMD 15 ps simulations. The plots of the distances of the Cu−Y bonds to be dissociated as a function

**Table 3. Possible Five- and Four-Coordinated Species Derived from Three Six-Coordinated Precursors of Type $[Cu(HG_1G_2G_3)(Py)(W)]$[a]**

| | equatorial ligands | | | | axial ligands | |
|---|---|---|---|---|---|---|
| **0** | **$N_H$** | **$N_{G1}$** | **$N_{G2}$** | **$O_{G2}$** | **$N_{Py}$** | **$O_W$** |
| **1** | | $N_{G1}$ | $N_{G2}$ | $O_{G2}$ | $N_{Py}$ | $O_W$ |
| **2** | $N_H$ | $N_{G1}$ | $N_{G2}$ | | $N_{Py}$ | $O_W$ |
| **3** | $N_H$ | $N_{G1}$ | $N_{G2}$ | $O_{G2}$ | | $O_W$ |
| **4** | $N_H$ | $N_{G1}$ | $N_{G2}$ | $O_{G2}$ | $N_{Py}$ | |
| **5** | | $N_{G1}$ | $N_{G2}$ | | $N_{Py}$ | $O_W$ |
| **6** | | $N_{G1}$ | $N_{G2}$ | $O_{G2}$ | | $O_W$ |
| **7** | | $N_{G1}$ | $N_{G2}$ | $O_{G2}$ | $N_{Py}$ | |
| **8** | $N_H$ | $N_{G1}$ | $N_{G2}$ | | | $O_W$ |
| **9** | $N_H$ | $N_{G1}$ | $N_{G2}$ | | $N_{Py}$ | |
| **10** | $N_H$ | $N_{G1}$ | $N_{G2}$ | $O_{G2}$ | | |
| | **$O_W$** | **$N_{G1}$** | **$N_{G2}$** | **$O_{G2}$** | **$N_{Py}$** | **$N_H$** |
| | | $N_{G1}$ | $N_{G2}$ | $O_{G2}$ | $N_{Py}$ | $N_H$ |
| | $O_W$ | $N_{G1}$ | $N_{G2}$ | | $N_{Py}$ | $N_H$ |
| | $O_W$ | $N_{G1}$ | $N_{G2}$ | $O_{G2}$ | | $N_H$ |
| | $O_W$ | $N_{G1}$ | $N_{G2}$ | $O_{G2}$ | $N_{Py}$ | |
| | | $N_{G1}$ | $N_{G2}$ | | $N_{Py}$ | $N_H$ |
| | | $N_{G1}$ | $N_{G2}$ | $O_{G2}$ | | $N_H$ |
| | | $N_{G1}$ | $N_{G2}$ | $O_{G2}$ | $N_{Py}$ | |
| | $O_W$ | $N_{G1}$ | $N_{G2}$ | | | $N_H$ |
| | $O_W$ | $N_{G1}$ | $N_{G2}$ | | $N_{Py}$ | |
| | $O_W$ | $N_{G1}$ | $N_{G2}$ | $O_{G2}$ | | |
| | **$N_{Py}$** | **$N_{G1}$** | **$N_{G2}$** | **$O_{G2}$** | **$O_W$** | **$N_H$** |
| | | $N_{G1}$ | $N_{G2}$ | $O_{G2}$ | $O_W$ | $N_H$ |
| | $N_{Py}$ | $N_{G1}$ | $N_{G2}$ | | $O_W$ | $N_H$ |
| | $N_{Py}$ | $N_{G1}$ | $N_{G2}$ | $O_{G2}$ | | $N_H$ |
| | $N_{Py}$ | $N_{G1}$ | $N_{G2}$ | $O_{G2}$ | $O_W$ | |
| | | $N_{G1}$ | $N_{G2}$ | | $O_W$ | $N_H$ |
| | | $N_{G1}$ | $N_{G2}$ | $O_{G2}$ | | $N_H$ |
| | | $N_{G1}$ | $N_{G2}$ | $O_{G2}$ | $O_W$ | |
| | $N_{Py}$ | $N_{G1}$ | $N_{G2}$ | | | $N_H$ |
| | $N_{Py}$ | $N_{G1}$ | $N_{G2}$ | | $O_W$ | |
| | $N_{Py}$ | $N_{G1}$ | $N_{G2}$ | $O_{G2}$ | | |

[a]The ligands defining the six-coordinated forms are reported in bold. The forms related to the first precursor **0** are labeled as **1**−**10**.

of the SMD simulation time are reported in Figure 2, and give a qualitative but very illuminating representation of the strength of the considered Cu−Y bond. Since the starting structure is the same for all bonds, and since the bonds are subjected to the same dissociative force (with the exception of the Cu−$N_H$ bond, see below), earlier in time the bond is dissociated and weaker is the bond. From Figure 2, it is clear that the Cu−$O_W$ is the weakest bond among all the coordination bonds in the complex: the corresponding distance reaches the upper limit of about 5 Å in less than 3 ps. The behavior of the Cu−$N_{Py}$ bond is analogous to that of Cu−$O_W$, but the dissociation occurs at a slightly longer time. The dissociation of the Cu−$O_{G2}$ bond takes a considerably longer time (the corresponding plot is slowly increasing) and becomes effective only after about 12 ps. Finally, the behavior of the Cu−$N_H$ bond is very peculiar, in the sense that a value for the scalar $F$ (eq 3) equal to that used for other bonds (0.005 hartree/bohr) does not induce dissociation, but only large-amplitude oscillations of the bond. Dissociation, on the contrary, can be induced only by a value of $F$ twice larger. From these results one can easily conclude that the strength of the coordination bonds follows the order Cu−$N_H$ > Cu−$O_{G2}$ > Cu−$N_{Py}$ > Cu−$O_W$.

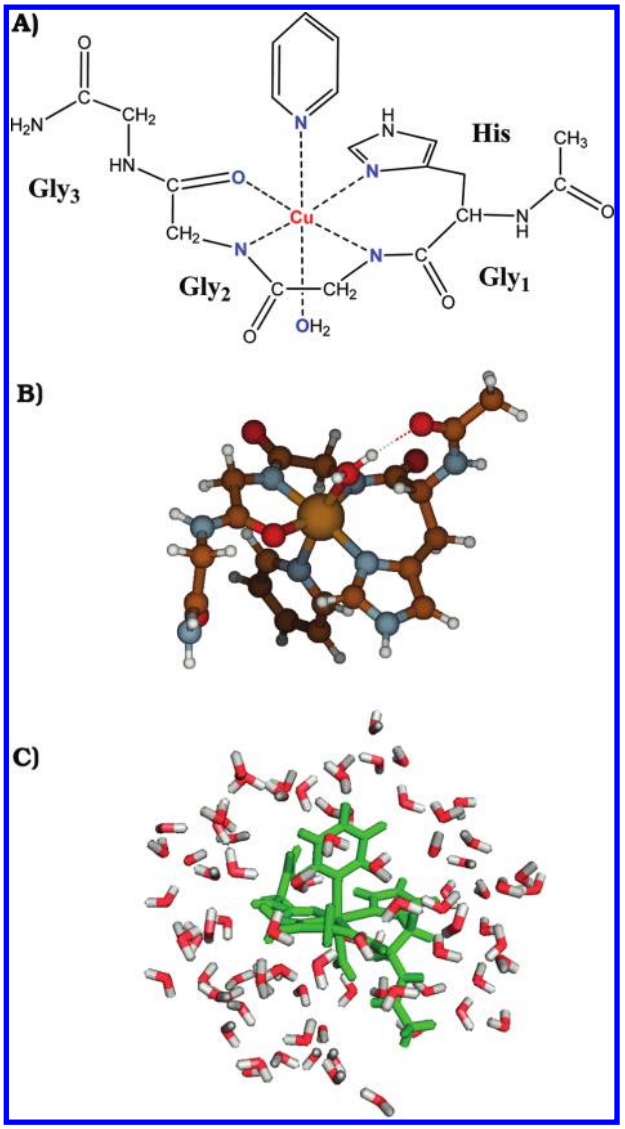


**Figure 1.** Complex $[Cu(AcHG_1G_2G_3NH_2)(Py)(W)]$ used as a precursor of all the five- and four-coordinated forms considered in this study. (A) Schematic representation of the complex; (B) molecular geometry of the complex alone; (C) the complex inserted into a sphere of 84 water molecules.

As described above, the four forms **1**−**4** have been also optimized at DFTB and DFT level, giving the final results reported in Table 4 (see below).

*Four-Coordinated Forms.* The four-coordinated forms are generated from the precursor **0** by dissociating two coordination bonds. This leads to six forms (**5**−**10**) characterized by the presence of the coordinated ligands reported in Table 3. The behavior of the pairs of bonds along the DFTB SMD trajectory is reported in Figure 3.

It should be noted that all the simulations concerning the dissociation of the Cu−$N_H$ bond have been carried out using a value of $F$ (eq 3) equal to 0.01 hartree/bohr, as done also for the corresponding simulation leading to the five-coordinated form. When comparing Figure 2 with Figure 3, one can observe that the behavior in time of the individual coordination bonds is very similar, thus confirming the rank of the relative stability of the bonds. The dissociation of the Cu−$O_W$ bond occurs always in the shortest time, followed in order by Cu−$N_{Py}$, Cu−$O_{G2}$, and Cu−$N_H$. The relative strengths of the bonds, determined


dx.doi.org/10.1021/jp210409c | J. Phys. Chem. B 2012, 116, 6250−6260

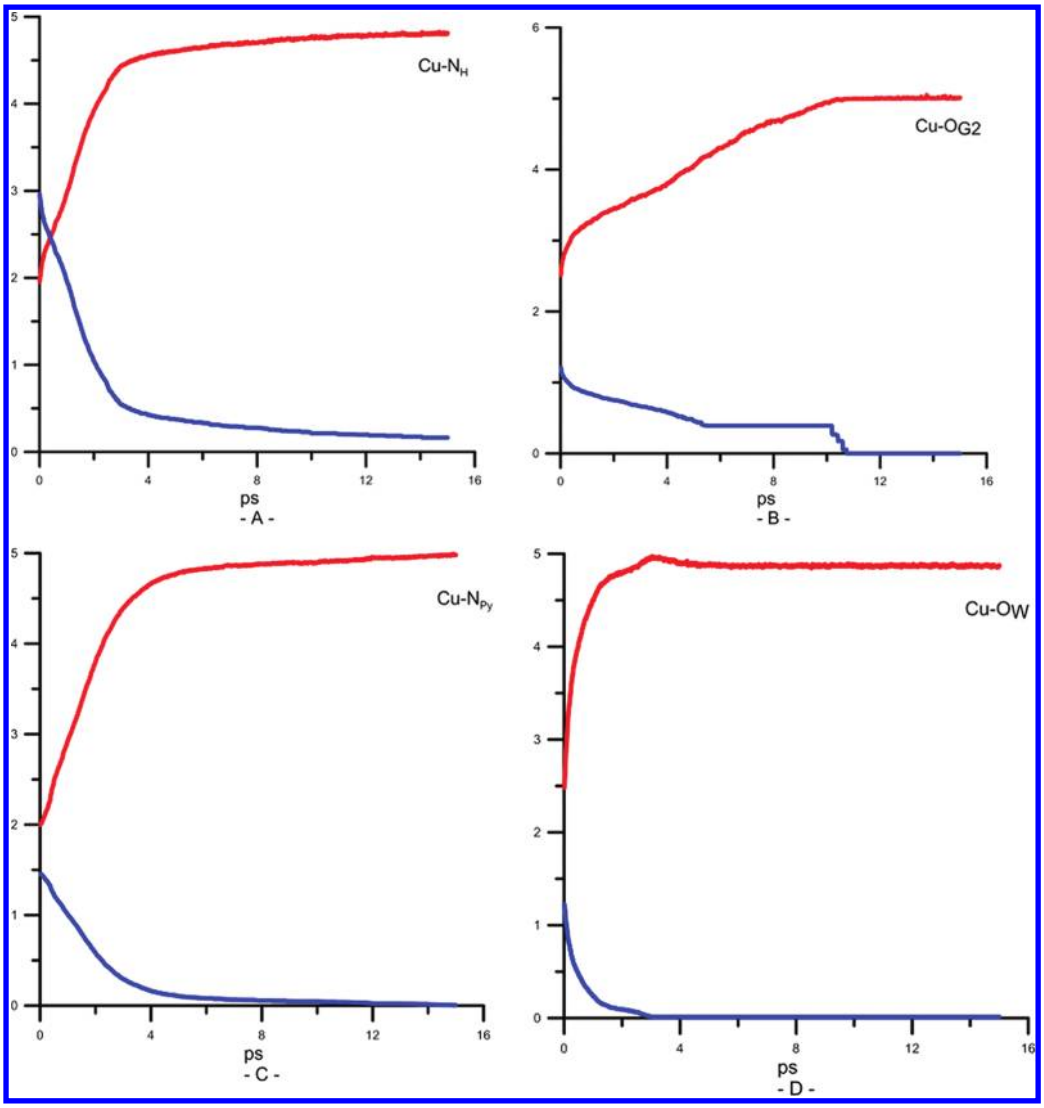


**Figure 2.** Cu−Y bond distances (Å, red) and the residual steering forces (meV/Å, blue) as functions of time along the SMD trajectory. Panels A, B, C, and D for the forms **1**, **2**, **3**, and **4**, respectively.

qualitatively on the basis of their time behavior, must correspond also to the stability of the isomers, as determined by the DFTB geometry optimization. This point will be discussed in detail in the following.

*Relative Stabilities of the [Cu(HG$_1$G$_2$G$_3$)(Py)(W)] Isomers.* As already described, the final DFTB-SMD configurations have been used as the starting points for DFTB and DFT optimizations leading to the results reported in Table 4, in which the relative stabilities are calculated from the energy values $E_C + E_{C-W}$ commented above. Using the optimized geometry, for each form **1**−**10** we have recomputed the Cu−Y distances associated with all the possible coordination bonds. The Cu−Y distances, which are (conventionally) considered too large to be representative of a coordination bond, are reported in Table 4 in bold. Therefore, the data of Table 4 give a very direct description of the type of coordination reached by geometry optimization, starting from a specific SMD final structure.

We first analyze the results of the DFTB optimizations. In general, the coordination feature obtained from DFTB optimization is always very close to that schematically given in Table 3. For instance, the optimized five-coordinated isomers **1**, **2**, **3**, and **4** have dissociated bonds Cu−N$_H$, Cu−O$_{G2}$, Cu−N$_{Py}$, and Cu−O$_W$, respectively. The same behavior is found for the six four-coordinated species. We conclude that the DFTB optimization does not induce important geometry rearrangement in the final structure of the DFTB-SMD trajectory. However, the DFTB optimization is necessary in order to remove completely the constraints potentially present in the DFTB-SMD simulations. As for the stability of the isomers, the best form is **4**, with the Cu−O$_W$ bond dissociated but with a pyridine molecule coordinated. The isomer **4** is followed by the isomer **10** ($\Delta E$ = 1.8 kcal mol$^{-1}$) which is a four-coordinated species CuN$_H$N$_{G1}$N$_{G2}$O$_{G2}$. A similar form is also produced for the isomer 3 ($\Delta E$ = 4.1 kcal mol$^{-1}$), but with the coordinating water molecule at a relatively low distance (about 2.7 Å).

The results of the full DFT (TZVP/BP86) geometry optimizations started from the last frame of the DFTB-SMD trajectories for the copper complex surrounded by 84 water molecules are reported for each isomer in Table 4, as the second entry. The agreement with the DFTB results is satisfactory, considering that for a such complex system (characterized by a very shallow potential energy surface) the


dx.doi.org/10.1021/jp210409c | J. Phys. Chem. B 2012, 116, 6250−6260

Table 4. DFTB and DFT Cu−Y Distances in Isomers 1−10 and Their Relative Stabilities[a]

| isomer | Cu−$N_H$ | Cu−$N_{G1}$ | Cu−$N_{G2}$ | Cu−$O_{G2}$ | Cu−$N_{Py}$ | Cu−$O_W$ | $\Delta E$ |
|---|---|---|---|---|---|---|---|
| **1** | **4.26** | 1.97 | 1.95 | 2.24 | 2.03 | 2.31 | 36.6 |
| | **4.02** | 2.06 | 1.94 | 2.12 | 2.25 | 2.00 | 23.3 |
| | **4.10** | 2.06 | 1.96 | 2.14 | 2.21 | 2.03 | 25.8 |
| **2** | 1.91 | 1.99 | 1.96 | **4.45** | 2.01 | 2.74 | 35.6 |
| | 1.97 | 2.01 | 1.98 | **3.54** | 2.06 | **4.73** | 25.9 |
| | 1.99 | 2.00 | 1.99 | **4.16** | 2.09 | **3.22** | 26.4 |
| **3** | 1.96 | 1.97 | 1.95 | 2.01 | **5.12** | 2.67 | 4.1 |
| | 1.97 | 2.01 | 1.94 | 2.12 | **6.73** | 3.97 | 4.9 |
| | 1.96 | 2.02 | 1.91 | 2.11 | **7.50** | **4.03** | 3.5 |
| **4** | 1.93 | 1.97 | 1.96 | 2.61 | 1.99 | **4.48** | 0.0 |
| | 1.97 | 2.06 | 1.95 | 2.32 | 2.20 | **4.14** | 0.0 |
| | 1.97 | 2.07 | 1.95 | 2.54 | 2.12 | **4.72** | 0.0 |
| **5** | **4.22** | 1.96 | 1.95 | **3.28** | 1.97 | 2.01 | 39.4 |
| | **3.99** | 1.95 | 1.98 | **3.28** | 2.02 | 2.07 | 27.9 |
| | **4.02** | 1.98 | 1.96 | **3.38** | 2.02 | 2.04 | 22.2 |
| **6** | **4.92** | 1.98 | 1.95 | 2.01 | **5.16** | 2.01 | 46.9 |
| | **5.54** | 2.02 | 1.89 | 2.06 | **4.27** | 1.98 | 15.0 |
| | **4.53** | 2.04 | 1.90 | 2.10 | **6.50** | 2.00 | 26.3 |
| **7** | **4.10** | 1.96 | 1.98 | 2.01 | 1.98 | **4.62** | 35.0 |
| | **3.47** | 1.99 | 1.93 | 2.07 | 2.01 | **4.40** | 37.5 |
| | **4.05** | 2.02 | 1.91 | 2.08 | 2.02 | **3.99** | 39.7 |
| **8** | 1.91 | 1.98 | 1.98 | **3.90** | **5.37** | 2.01 | 37.5 |
| | 1.98 | 1.96 | 1.96 | **3.64** | **7.38** | 2.08 | 33.2 |
| | 1.98 | 1.99 | 1.93 | **3.61** | **4.96** | 2.19 | 28.8 |
| **9** | 1.95 | 1.98 | 1.97 | **4.03** | 1.99 | **4.58** | 19.2 |
| | 1.98 | 2.00 | 1.96 | **3.82** | 2.07 | **3.80** | 26.9 |
| | 2.00 | 1.99 | 1.96 | **3.65** | 2.06 | **3.91** | 30.5 |
| **10** | 1.96 | 1.99 | 1.96 | 2.01 | **4.94** | **4.26** | 1.8 |
| | 1.96 | 2.05 | 1.91 | 2.12 | **5.76** | **5.08** | 1.4 |
| | 1.95 | 2.05 | 1.92 | 2.11 | **5.83** | **4.39** | 1.1 |

[a]DFTB, TZVP/BP86 with 84 water molecules, and TZVP/BP86 with 40 water molecules in first, second, and third entry, respectively. Distances in Å. The distances between the copper atom and noncoordinated ligands (dissociated bonds) are reported in bold. $\Delta E$ are the relative stabilities in kcal·mol$^{-1}$.

number of possible local minima is extremely high. This can easily explain the (relatively) small differences in the best bound distances among the DFTB and the DFT isomers. Notably, we observe that the sequence in stability predicted by DFTB calculations for the lowest energy isomers is nicely confirmed by the DFT ones. In particular, the DFT geometry optimization of isomer **3** shows that the dissociation of the Py ligand is followed also by the loss of the coordination of the axial water molecule, as found by DFTB, even if this approach predicts a stronger interaction of the axial water molecule with the $Cu^{2+}$ ion than the DFT approach.

Finally, in order to prove the role played by the size of the solvation sphere we have also performed DFT optimizations of systems composed by the copper complex and only 40 water molecules. Such systems have been derived from the corresponding models with 84 water molecules by simply deleting the water molecules having a distance from the copper atom larger than (about) 7.7 Å. The previously commented DFTB and DFT results are fairly reproduced also by the reduced hydration sphere. This result is very important because at DFT level (the most time consuming step in the speciation process) this can represent a substantial save of computational time.

## 4. CONCLUSIONS

All the results commented above allow to conclude that in the presence of pyridine the lowest energy isomer is the five-coordinated form $CuN_HN_{G1}N_{G2}O_{G2}N_{Py}$. To this conclusion converge, with substantial agreement, DFTB and DFT-TZVP results, the last including both 84 and 40 water molecules. This agreement represents a very encouraging result for a large-scale application of our computational protocol in the study of speciation of other copper−peptide systems. It should be stressed that DFTB and DFT results agree as for the sequence of the three lowest energy isomers, namely **4**, **10**, and **3**, respectively. All the results obtained in the present study also allow to draw the following general conclusions, which are relevant from a methodological point of view. The optimization of the Cu−Y (Y = H, C, N, O) potentials which has been carried out in this study could be even further refined by considering explicitly the formation energies of the Cu−Y bonds. This could further improve the predictive capability of the DFTB approach. The DFTB computational protocol here presented can be considered as very satisfactory, at least in the sense of being able of selecting the most stable isomers, among which the more accurate DFT method could formulate a reliable rank of stability. The full study of the speciation of the $[Cu(HG_1G_2G_3)(Py)(W)]$ complex in water solution, in the presence or absence of an extra pyridine ligand, will be presented in a forthcoming paper.


dx.doi.org/10.1021/jp210409c | J. Phys. Chem. B 2012, 116, 6250−6260

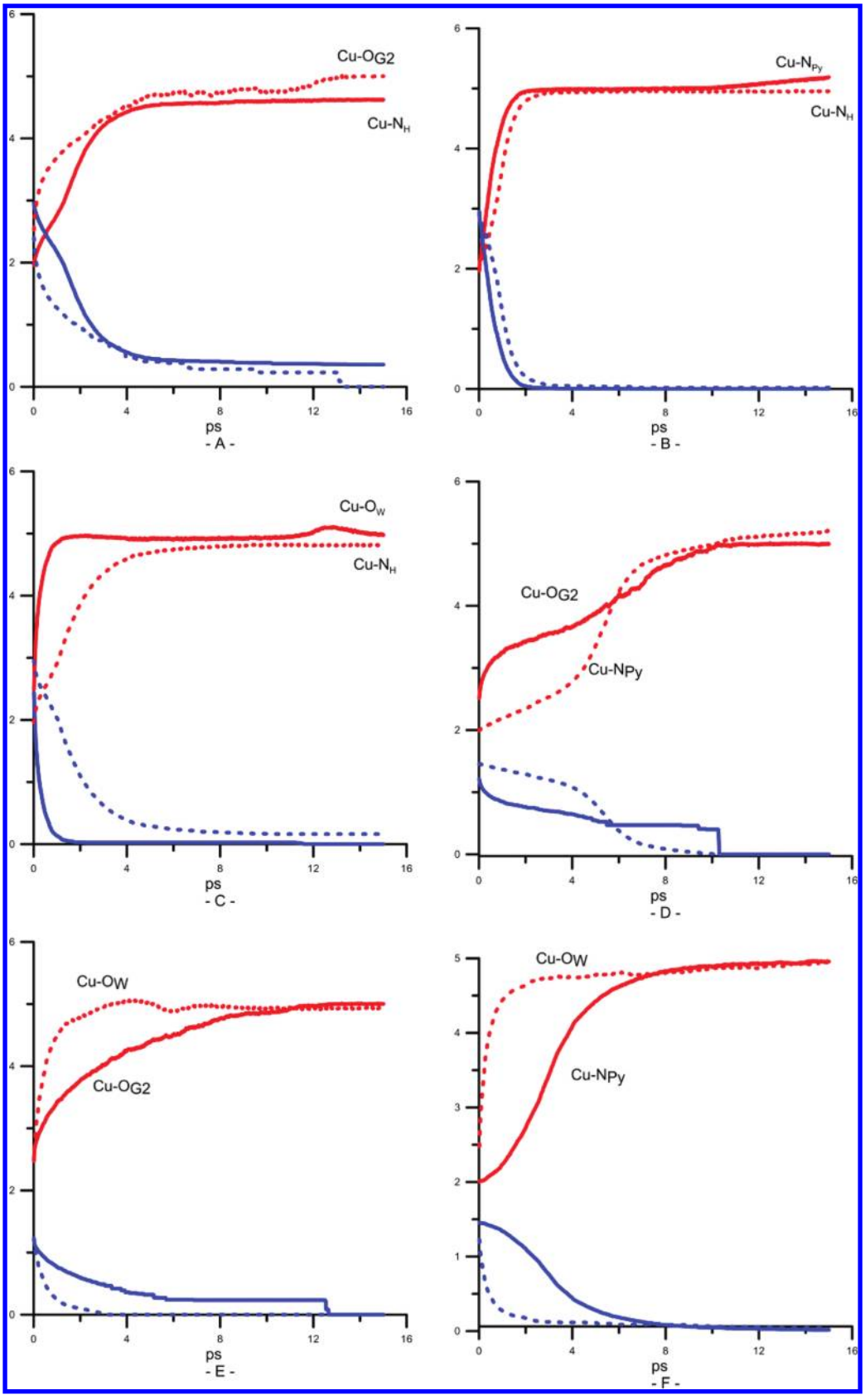


**Figure 3.** Cu−Y (full lines) and Cu−Y′ (dotted lines) bond distances (Å, red) and residual steering forces (meV/Å, blue) as function of time, along the DFTB SMD trajectory. Panels A, B, C, D, E, and F for the forms **5**, **6**, 7, **8**, **9**, and **10**, respectively.


dx.doi.org/10.1021/jp210409c | *J. Phys. Chem. B* 2012, 116, 6250−6260

## AUTHOR INFORMATION


### Corresponding Author

*E-mail: piercarlo.fantucci@unimib.it (P.F.); maurizio.bruschi@unimib.it (M.B.). Tel.: +39-0264483477 (P.F.); +39-0264482816 (M.B.). Fax: +39-0264483478 (P.F.); +39-0264482890 (M.B.).


### Notes

The authors declare no competing financial interest.

## ACKNOWLEDGMENTS

This work was supported by the PRIN Project no. 200875WHMR.

## REFERENCES


(1) Freeman, H. C. *Adv. Protein Chem.* **1967**, *22*, 257.
(2) Sigel, H.; Martin, R. B. *Chem. Rev.* **1982**, *82*, 385.
(3) Xing, G.; DeRose, V. J. *Curr. Opin. Chem. Biol.* **2001**, *5*, 196.
(4) Burns, C. S.; Aronoff-Spencer, E.; Dunham, C. M.; Lario, P.; Avdievich, N. I.; Antholine, W. E.; Olmstead, M. M.; Vrielink, A.; Gerfen, G. J.; Peisach, J.; Scott, W. G.; Millhauser, G. L. *Biochemistry* **2002**, *41*, 3991.
(5) Pogni, R.; Dellalunga, G.; Basosi, R. *J. Am. Chem. Soc.* **1993**, *115*, 1546.
(6) Gajda, T.; Henry, B.; Delpuech, J. J. *J. Chem. Soc., Dalton Trans.* **1993**, 1301.
(7) Sanna, D.; Ágoston, C. G.; Sóvágo, I.; Micera, G. *Polyhedron* **2001**, *20*, 937.
(8) Bonomo, R. P.; Impellizzeri, G.; Pappalardo, G.; Rizzarelli, E.; Tabbì, G. *Chem.—Eur. J.* **2000**, *6*, 4195.
(9) Bonomo, R. P.; Cucinotta, V.; Giuffrida, A.; Impellizzeri, G.; Magrì, A.; Pappalardo, G.; Rizzarelli, E.; Santoro, A. M.; Tabbì, G.; Vagliasindi, L. *J. Chem. Soc., Dalton Trans.* **2005**, 150.
(10) Bonomo, R. P.; Pappalardo, G.; Rizzarelli, E.; Tabbì, G.; Vagliasindi, L. I. *Dalton Trans.* **2008**, 3805.
(11) Stewart, J. J. P. *J. Mol. Model.* **2007**, *13*, 1173.
(12) Elstner, M.; Porezag, D.; Jungnickel, G.; Elsner, J.; Haugk, M.; Frauenheim, T.; Suhai, S.; Seifert, G. *Phys. Rev. B* **1998**, *58*, 7260.
(13) Frauenheim, T.; Seifert, G.; Elstner, M.; Hajnal, Z.; Jungnickel, G.; Porezag, D.; Suhai, S.; Scholz, R. *Phys. Status Solidi B* **2000**, *217*, 41.
(14) Köhler, C.; Seifert, G.; Gerstmann, U.; Elstner, M.; Overhof, H.; Frauenheim, T. *Phys. Chem. Chem. Phys.* **2001**, *3*, 5109.
(15) Aradi, B.; Hourahine, B.; Frauenheim, T. *J. Phys. Chem. A* **2007**, *111*, 5678.
(16) Elstner, M. *J. Phys. Chem. A* **2007**, *111*, 5614.
(17) Moreira, N. H.; da Rosa, A. L.; Frauenheim, T. *Appl. Phys. Lett.* **2009**, *94*.
(18) Milosevic, I.; Nikolic, B.; Dobardzic, E.; Damnjanovic, M.; Popov, I.; Seifert, G. *Phys. Rev. B* **2007**, *76*.
(19) Rasche, B.; Seifert, G.; Enyashin, A. *J. Phys. Chem. C* **2010**, *114*, 22092.
(20) Dolgonos, G.; Aradi, B.; Moreira, N. H.; Frauenheim, T. *J. Chem. Theory Comput.* **2010**, *6*, 266.
(21) Trani, F.; Barone, V. *J. Chem. Theory Comput.* **2011**, *7*, 713.
(22) Nakamura, K.; Arita, R.; Ikeda, H. *Phys. Rev. B* **2011**, *83*.
(23) Ivanovskii, A. L.; Enyashin, A. N. *Chem. Phys. Lett.* **2011**, *509*, 143.
(24) Elstner, M.; Frauenheim, T.; Kaxiras, E.; Seifert, G.; Suhai, S. *Phys. Status Solidi B* **2000**, *217*, 357.
(25) Elstner, M. *Theor. Chem. Acc.* **2006**, *116*, 316.
(26) Riccardi, D.; Schaefer, P.; Yang, Y.; Yu, H. B.; Ghosh, N.; Prat-Resina, X.; Konig, P.; Li, G. H.; Xu, D. G.; Guo, H.; Elstner, M.; Cui, Q. *J. Phys. Chem. B* **2006**, *110*, 6458.
(27) Hobza, P.; Kubar, T.; Jurecka, P.; Cerny, J.; Rezac, J.; Otyepka, M.; Valdes, H. *J. Phys. Chem. A* **2007**, *111*, 5642.
(28) Goyal, P.; Ghosh, N.; Phatak, P.; Clemens, M.; Gaus, M.; Elstner, M.; Cui, Q. *J. Am. Chem. Soc.* **2011**, *133*, 14981.
(29) Morokuma, K.; Lundberg, M.; Sasakura, Y.; Zheng, G. S. *J. Chem. Theory Comput.* **2010**, *6*, 1413.
(30) Guo, H.; Xu, D. G.; Cui, Q. *J. Phys. Chem. A* **2007**, *111*, 5630.
(31) Elstner, M.; Cui, Q.; Munih, P.; Kaxiras, E.; Frauenheim, T.; Karplus, M. *J. Comput. Chem.* **2003**, *24*, 565.
(32) Xu, D.; Xie, D.; Guo, H. *J. Biol. Chem.* **2006**, *281*, 8740.
(33) Xu, D.; Guo, H. *J. Am. Chem. Soc.* **2009**, *131*, 9780.
(34) Riccardi, D.; Konig, P.; Guo, H.; Cui, Q. *Biochemistry* **2008**, *47*, 2369.
(35) Riccardi, D.; Yang, S.; Cui, Q. *Biochim. Biophys. Acta* **2010**, *1804*, 342.
(36) Wu, S.; Zhang, C.; Xu, D.; Guo, H. *J. Phys. Chem. B* **2010**, *114*, 9259.
(37) Wu, S.; Zhang, C.; Cao, R.; Xu, D.; Guo, H. *J. Phys. Chem. B* **2011**, *115*, 10360.
(38) Franzini, E.; De Gioia, L.; Fantucci, P.; Zampella, G.; Bonačić-Koutecký, V. *Inorg. Chem. Commun.* **2003**, *6*, 650.
(39) Riihimäki, E. S.; Kloo, L. *Inorg. Chem.* **2006**, *45*, 8509.
(40) Marino, T.; Russo, N.; Toscano, M. *J. Phys. Chem. B* **2007**, *111*, 635.
(41) Pushie, M. J.; Rauk, A. *J. Biol. Inorg. Chem.* **2003**, *8*, 53.
(42) Furlan, S.; Penna, G.; Guerrieri, F.; Morante, S.; Rossi, G. C. *J. Biol. Inorg. Chem.* **2007**, *12*, 571.
(43) Bruschi, M.; De Gioia, L.; Mitrić, R.; Bonačić-Koutecký, V.; Fantucci, P. *Phys. Chem. Chem. Phys.* **2008**, *10*, 4573.
(44) Brown, D. R.; Qin, K.; Herms, J. W.; Madlung, A.; Manson, J.; Strome, R.; Fraser, P. E.; Kruck, T.; von Bohlen, A.; Schulz-Schaeffer, W.; Giese, A.; Westaway, D.; Kretzschmar, H. *Nature* **1997**, *390*, 684.
(45) Stöckel, J.; Safar, J.; Wallace, A. C.; Cohen, F. E.; Prusiner, S. B. *Biochemistry* **1998**, *37*, 7185.
(46) Pauly, P. C.; Harris, D. A. *J. Biol. Chem.* **1998**, *273*, 33107.
(47) Bonomo, R. P.; Pappalardo, G.; Rizzarelli, E.; Santoro, A. M.; Tabbi, G.; Vagliasindi, L. I. *Dalton Trans.* **2007**, 1400.
(48) Luczkowski, M.; Kozlowski, H.; Stawikowski, M.; Rolka, K.; Gaggelli, E.; Valesin, D.; Valesin, G. *J. Chem. Soc., Dalton Trans.* **2002**, 2269.
(49) Mentler, M.; Weiss, A.; Grantner, K.; del Pino, P.; Deluca, D.; Fiori, S.; Renner, C.; Klaucke, W. M.; Moreder, L.; Bertsch, U.; Kretzschman, H. A.; Tavan, P.; Parak, F. G. *Eur. Biophys. J.* **2004**, *34*, 97.
(50) Brown, D. R.; Kozlowski, H. *J. Chem. Soc., Dalton Trans.* **2004**, 1907.
(51) Krüger, T.; Elstner, M.; Schiffels, P.; Frauenheim, T. *J. Chem. Phys.* **2005**, *122*, 114110.
(52) Becke, A. D. *Phys. Rev. A* **1988**, *38*, 3098.
(53) Perdew, J. P. *Phys. Rev. B* **1986**, *33*, 8822.
(54) Schäfer, A.; Huber, C.; Ahlrichs, R. *J. Chem. Phys.* **1994**, *100*, 5829.
(55) R.; Bar, M.; Haser, M.; Horn, H.; Kolmel, C. *Chem. Phys. Lett.* **1989**, *162*, 165.
(56) Morokuma, K.; Zheng, G. S.; Witek, H. A.; Bobadova-Parvanova, P.; Irle, S.; Musaev, D. G.; Prabhakar, R. *J. Chem. Theory Comput.* **2007**, *3*, 1349.
(57) Niehaus, T. A.; Elstner, M.; Frauenheim, T.; Suhai, S. *J. Mol. Struct.: Theochem* **2001**, *541*, 185.
(58) Szu, M.; Hartley, R. *Phys. Lett. A* **1987**, *122*, 157.
(59) (a) Roos, B.; Salez, C.; Veillard, A.; Clementi, E. *IBM Res. Rep.* **1968**, *RJ*, 518. (b) Clementi, E.; Chakravorty, S. J.; Corongiu, G.; Flores, J. R.; Sonnad, V. In *Modern techniques in computational chemistry (MOTECC-91)*; Clementi, E., Ed.; ESCOM: Leiden, The Netherlands, 1991; pp 23−14.
(60) Perdew, J.; Burke, K.; Ernzerhof, M. *Phys. Rev. Lett.* **1996**, *77*, 3865.
(61) Perdew, J.; Burke, K.; Ernzerhof, M. *Phys. Rev. Lett.* **1997**, *78*, 1396.
(62) Becke, A. D. *J. Chem. Phys.* **1993**, *98*, 5648.
(63) Sabolović, J.; Tautermann, C. S.; Loerting, T.; Liedl, K. R. *Inorg. Chem.* **2003**, *42*, 2268.
(64) Dewar, M. J. S.; Jie, C.; Yu, J. *Tetrahedron* **1993**, *49*, 5003.

(65) Holder, A. J.; Dennington, R. D.; Jie, C. *Tetrahedron* **1994**, *50*, 627.
(66) Semichem, Inc.: PO Box 1649, Shawnee, KS 66222, 1994−2002.
(67) Maxcy, K. R.; Turnbull, M. M. *Acta Crystallogr. C* **1999**, *55*, 1986.
(68) Lebrun, P. C.; Lyon, W. D.; Kuska, H. A. *J. Crystallogr. Spectrosc. Res.* **1986**, *16*, 889.
(69) Freeman, H. C.; Snow, M. R.; Nitta, I.; Tomita, K. *Acta Crystallogr.* **1964**, *17*, 1463.